Available online at www.sciencedirect.com
ScienceDirect
International Journal of Mass Spectrometry 262 (2007) 154–160
International Journal of Mass Spectrometry
www.elsevier.com/locate/ijms

Ionizing fragmentation of uracil and 5-bromouracil by electron impact in gas phase and hyperthermal Ar^+ ion irradiation in condensed phase

Marjorie Imhoff, Zongwu Deng, Michael A. Huels *

Ion Reaction Laboratory, Department of Nuclear Medicine and Radiobiology, Faculty of Medicine and Health Sciences, University of Sherbrooke, Sherbrooke, Quebec, J1H 5N4 Canada

Received 16 October 2006; received in revised form 6 November 2006; accepted 7 November 2006
Available online 8 December 2006

Abstract

The chemical composition and formation channels of charged fragments of uracil (U) and 5-bromouracil (BrU) produced by 70 eV electron impact in gas phase and 10–200 eV Ar^+ ion irradiation in condensed phase are investigated in parallel with that of thymine (T). This is part of our effort to unravel possible different molecular level mechanisms of DNA damage caused by heavy ion radiation and the radiosensitivity of 5-BrU observed during UV, X- and γ-ray radiation. Abundant ionic fragments are produced from the three molecules by both electron impact and ion irradiation through similar bond-breaking channels due mainly to their very similar molecular structures. During electron impact major cation fragments are identified as $[M - OCNH]^+$, $NHCHCCH_3^+$(T)/$NHCHCH^+$(U)/$NHCHCBr^+$(BrU), $OCNH_2^+$, $HNCH^+/CO^+$, $C_xH_y^+$ ($x = 1$–3; $y = 0$–4), etc. and a parent cation $[M]^+$ as well where M = T, U or 5-BrU. During ion irradiation some of these fragments partially or completely appear in their protonated forms, and an additional cation fragment $[M - O]^+$ is also observed. Major anion fragments produced by ion irradiation are H^-, O^-, CN^-, OCN^- for all three molecules with trace amount of hydrocarbon anions. An additional Br^- anion is produced for 5-BrU. The parent anions are discernable in their deprotonated forms only from very thin films. During Ar^+ ion irradiation, fragment desorption begins at incident ion energies down to 20 eV. Anion fragment desorption appears at much higher energies at around 40 eV, and strongly depends on the film thickness.

Keywords: Nucleobase; Electron & ion impact; Fragmentation; Gas phase; Condensed phase

1. Introduction

5-Bromouracil (BrU) is not normally found in DNA but it can be substituted for thymine and incorporated in DNA during replication. Incorporation of 5-BrU into DNA leads to two important properties of biological significance, i.e., mutagenesis and radiosensitivity. First, it induces a substitution-type mutation of A–T to G–C [1]. Second, when 5-BrU is incorporated into cellular DNA in place of thymine, cells become much more sensitive to the lethal effects of UV, X-ray and γ-ray radiation [2]. This sensitization is due to the fact that 5-BrU, and other 5-halouracils (e.g., 5-IU) in general, are much more radiation sensitive than the normal bases. This has led to clinical trials of 5-BrU combined with radiation therapy [3].

This radiosensitivity has been attributed to the formation of an extremely reactive uracilyl radical by cleaving the C–Br bond [4], but the underlying molecular mechanism of 5-BrU in radiosensitivity is virtually not fully understood. It appears to be dependent on the radiation modality [5–14]. The most intensively studied case is UV radiation, where photo-stimulated electron transfer to 5-BrU from its adjacent 5′-nucleotide creates a BrU^- anion and a cationic base. The BrU^- anion then undergoes homolysis to yield a Br^- anion and an uracilyl-5-yl radical. The latter abstracts hydrogen from the sugar moiety of the adjacent 5′-nucleotide, and initiates DNA damage. The damage exhibits strong dependence on DNA structure and base sequence [5–10]. Dissociative electron attachment mechanism may play a role in all radiation modalities where low energy secondary electrons are produced in large numbers [11,12]. These two mechanisms both involve negative ionization of 5-BrU. In the cases of X- and γ-ray radiation, direct (positive) ionization has to be involved, and the damage pattern exhibits some different characteristics in terms of, e.g., its sequence dependence on single-stranded and duplex DNA [13,14].

Recently, it was revealed that heavy ion radiation track can produce secondary ions/fragments with kinetic energies from

* Corresponding author. Tel.: +1 819 346 1110x14907; fax: +1 819 564 5442.
E-mail address: michael.huels@USherbrooke.ca (M.A. Huels).

1387-3806/$ – see front matter © 2006 Elsevier B.V. All rights reserved.
doi:10.1016/j.ijms.2006.11.004

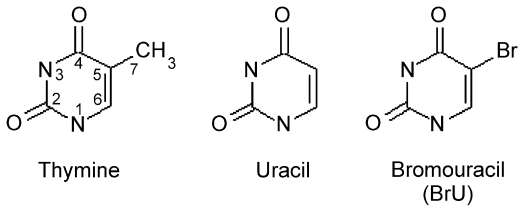

Fig. 1. Molecular structure of thymine, uracil, and 5-bromouracil.

thermal up to several hundreds eV in a biological medium [15–17], and in the subsequent scattering events these energetic ions/fragments can also cause severe damage to DNA. The latter is demonstrated by the complete disintegration of DNA components (nucleoside thymidine, base thymine, and the two sugar molecules D-ribose and 2-deoxy-D-ribose) and the scattering reactions induced by hyperthermal ion irradiation [18–23]. For example, ions induce molecular fragmentation at energies down to 10 eV [18], and various scattering reactions at energies down to nearly 0 eV [19,20].

This raises a question as of what happens when 5-BrU is incorporated into DNA molecules and then subjected to heavy ion radiation. In this work, we investigate the physical effects of the energetic secondary fragments on 5-BrU, i.e., fragmentation of 5-BrU by hyperthermal (10–200 eV) Ar^+ ions. Because both 5-BrU and thymine can be regarded as derivatives of uracil (a RNA base) by replacing its H atom on C5 with a Br atom or a methyl group (Fig. 1), the results will be presented here by comparing with those of thymine (T) and uracil (U). We examine the difference and similarity in bond breaking patterns induced by 10–200 eV Ar^+ ion irradiation in the condensed phase and 70 eV electron impact in the gas phase through identifying the chemical composition and formation channels of the fragments.

While direct ionization of 5-BrU can be studied by photon or electron impact in gas phase, in the condensed phase which mimicks a real biological medium better than gas phase, the lack of kinetic energy impedes the desorption of fragments and makes it difficult to observe high mass fragments. This problem can be tackled by using hyperthermal ions which transfer some kinetic energies to the resultant fragments and allow observation of abundant high mass ionic fragments from condensed phase (films). In this respect, singly charged hyperthermal ions used under our conditions cause fragmentation via valence (positive) ionization, much like positive ionization caused by low energy (e.g., 70 eV) electrons. This is demonstrated in the similar fragmentation patterns caused by electron ionization in gas phase and hyperthermal ion radiation in condensed phase [21]. Hence, on one hand, the results from ion studies also have implication for electron (positive) ionization in condensed phase. On the other hand, comparing results between ionizing fragmentation in gas phase and condensed phase can shed some light into the secondary events that may occur following ionization and fragmentation in a real biological medium.

2. Experimental method

The experiments were carried out on an ultrahigh-vacuum low energy ion beam reaction apparatus with a base pressure of 10^{-9} Torr. The apparatus will be described in detail elsewhere [24]. It consists of a low energy ion beam system, a molecular film preparation and monitoring system, and a quadrupole mass spectrometer (QMS, Hiden Analytical Ltd.) for product detection. Here we give a brief description on the experimental procedure used for the present study. The ion beam system delivers an Ar^+ ion beam of 10–500 eV at a nearly fixed current of ~30 nA into a reaction chamber for sample irradiation. The beam is focused at the target to a 2–4 mm spot. The energy spread of the cation beams is measured to be ~1 eV full width at half maximum.

The mass spectrometer is installed perpendicularly to the axis of the ion beam in the reaction chamber. It detects desorbing ionic products with *in vacuo* energies between 0 and 5 eV. During experiments the monoenergetic ion beam impinges on the target in the reaction chamber at an incident angle of 60°, and the desorbing ionic products are monitored by the QMS at a desorption angle of 30°, both with respect to the target surface normal. The mass spectrometer is used in two different modes: in the ion count mode the energy of the incident ions is held fixed and the desorption of ionic fragments is surveyed as a function of the ion mass. To determine the appearance energy threshold of a certain ionic fragment its intensity is monitored as a function of incident Ar^+ ion energy.

Films of thymine, uracil and 5-BrU were prepared via vacuum evaporation and condensation on a polycrystalline Pt foil substrate held at room temperature. The molecules, purchased from Aldrich without further purification, were loaded into a miniature oven in a loadlock chamber and degassed for several hours well below their evaporation onsets before experiments. During experiments the oven is heated to an appropriate temperature (90–100 °C for thymine and uracil, and 110–120 °C for 5-BrU, respectively) to yield an appropriate molecular deposition rate. The deposition rate is monitored by a movable quartz crystal microbalance in the loadlock chamber, and characterised in nanogram (ng)/cm^2 min. The microbalance has a sensitivity of 2 ng/cm^2. When a certain deposition rate is achieved and sustained, the oven is transferred into the reaction chamber and located at ~1 cm from the Pt surface to allow the molecules to condense on the substrate. The film thickness is determined by the known deposition rate and time. After preparation the film is brought swiftly to the irradiation location and subjected to ion irradiation, the desorption of ionic fragments is monitored.

Ion interaction with films of the three studied nucleobase molecules exhibits a significant dependence on the film thickness [23]. This is in contrast to the sugar molecular films where no such dependence on film thickness is observed [24]. The difference is currently ascribed to the change of surface work function and/or the presence or absence of a local charging effect on the molecular films. A slight charging of a thin base molecular film reduces anion fragment desorption, but is in favour of cation fragment desorption. Severer charge accumulation in a thick film may then impose much kinetic energy to the cation fragments such that they carry energy beyond the detection range of the mass spectrometer (0–5 eV). Here we find that films of 100–400 ng/cm^2 provide a good thickness range for measuring both positive and negative ion desorption. Based on the known

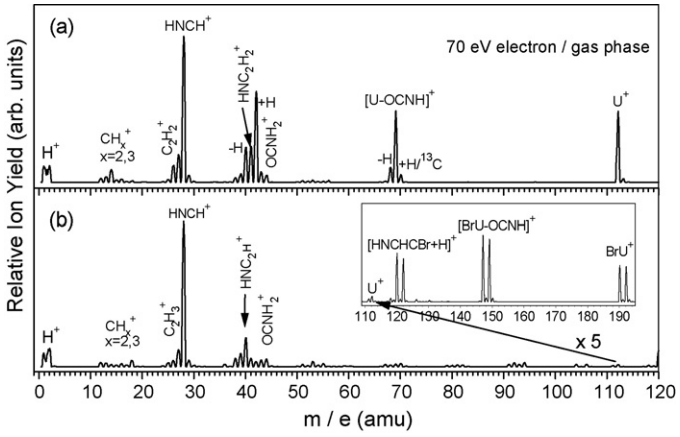

Fig. 2. *Cation* fragment patterns of (a) uracil and (b) 5-BrU produced by 70 eV electron impact in gas phase. In both mass spectra the relative intensity of the mass peaks has been normalized to their integral intensity of all fragments. The cation mass spectrum of 5-BrU is completed up to 200 amu in its inset (5×). Here in (a) and (b) the cation signal at 28 amu contains both HNCH and CO fragments (see text).

density, this thickness range corresponds roughly to 2–8 *nominal* monolayers in the case of thymine, assuming no clustering of the molecules.

Fragmentation patterns of the molecules induced by 70 eV electron impact were collected by using a built-in ionizer in the QMS after careful baking of the vacuum system to reduce background signal, as described elsewhere for the studies on thymine [21]. A relatively large amount of molecules are evaporated to the Pt substrate, which is then placed in front of the QMS. Subsequently, the molecules are gently evaporated again into the QMS by warming up the Pt substrate. A background spectrum, taken immediately prior to the sample evaporation, has been subtracted from the electron impact mass spectra presented here.

3. Results and discussion

Fig. 2 shows *cation* mass patterns of (a) uracil and (b) 5-BrU produced by 70 eV electron impact in gas phase. The results of thymine has been presented and discussed in great detail elsewhere [21]. Here we focus on the results of uracil and 5-BrU but shall frequently cite the results on thymine. The chemical identification of the fragments is accomplished by comparing with mass spectra of thymine and partially deuterated thymine [21], and is labeled in the spectra. Its discussion is given below and follows from large *m/e* to small *m/e* fragments. First, the molecular parent cations are seen at *m/e* 112 amu for U^+ and (190, 192) amu for BrU^+ (inset), respectively. The duplex peak of BrU^+ is due to the natural isotopic abundance of bromine (50.69% for ^{79}Br and 49.31% for ^{81}Br), which is a general feature of any fragments containing Br. The natural ^{13}C isotope also contributes to many tiny peaks adjacent to major fragments with one additional amu, depending on the number of carbon atom of the fragment, e.g., ∼4% for both U^+ at 113 amu and BrU^+ at 191, 193 amu.

The next large *m/e* fragment corresponds to loss of an OCNH group ($[M - OCNH]^+$, M = T, U, or 5-BrU) from the molecules. In order to facilitate correlating the chemical composition and formation channels of the fragments, the *m/e* values of some typical fragments with their individual formation pathways are listed in Table 1 along with that produced by ion impact (in parentheses). Loss of an OCNH group produces fragments at 82, 83 amu for thymine, 68, 69 amu for uracil, and 147, 149 amu for 5-BrU, respectively. There are three possible pathways of losing a OCNH group for all the three molecules, but they are not resolvable by the current study. The lost OCNH group can appear as $OCNH^+/OCNH_2^+$ or OCN^- fragments as will be discussed later.

Bond cleavage along N1–C2 and C4–C5 (Fig. 1) produces fragments $HNC_3H_3^+$, $HNC_3H_4^+$ (54, 55 amu) from thymine, $HNC_2H_2^+[\pm H]$ (40–42 amu) from uracil and $[HNC_2HBr + H]^+$ (120, 122 amu) from 5-BrU. Hydrogen loss or gain yields the two adjacent peaks at 40 and 42 amu for uracil, and $HNC_3H_3^+$ for thymine. It is somewhat surprising that the fragments produced from gas phase uracil and 5-BrU through this channel appear mainly (U) or completely (5-BrU) with one additional hydrogen. In the case of 5-BrU, the HNC_2HBr^+ fragment can further lose a Br atom to appear as HNC_2H^+ at 40 amu. Contribution to the 41 amu peak of uracil from a possible OC_2H^+ fragment and to the 120 and 122 amu peaks of 5-BrU from another possible fragment OC_2BrH^+ (through bond cleavage along C3–C4 and C5–C6) is likely negligible as in the case of thymine [21]. Instead, the latter appears as a weak OC_2Br^- anion when thin 5-BrU films are irradiated (see Fig. 4). Also noteworthy is that formation of U^+ or $[U - H]^+$ from 5-BrU is negligible.

According to the results of thymine [21], the strongest mass peak at 28 amu is likely a combination of both CO^+ and $HNCH^+$ fragments for all the three molecules. The latter is a result of bond cleavage along N1–C2 and C5–C6 of the relevant molecules. The tiny peak at 29 amu is originated mainly from natural ^{13}C isotope

Table 1
m/e values (in amu) of molecular fragments after picking up (+) or losing (−) specific atom/group from thymine (T), uracil (U) and 5-bromouracil (5-BrU)

Molecule (M)	Fragments					
	$M^+/[M+H]^+$	$[M-O]^+$	$[M-OCNH]^+$	$[HNCHCG7]^+$	$HNCH^+$	$[M-H]^-$
T	126 (127)	Nil (110)	82, 83 (82–84)	54, 55-CH_3 (54–56)	28 (28)	(125)
U	112 (113)	Nil (96)	68, 69 (68–70)	40–42-H (40–43)	28 (28)	(111)
5-BrU	190, 192 (191, 193)	Nil (174–177)	147, 149 (147–150)	120, 122-Br (120, 122)	28 (28)	(189, 191)

For each molecule, the values are the observed mass peak positions, in amu, of relevant fragments produced by 70 eV electron impact in the gas phase, and those in parentheses are the observed peak positions produced by hyperthermal ion irradiation in the condensed phase. G7 represents the group attached to carbon C5 of a molecule as indicated after the dash (refer to Fig. 1).

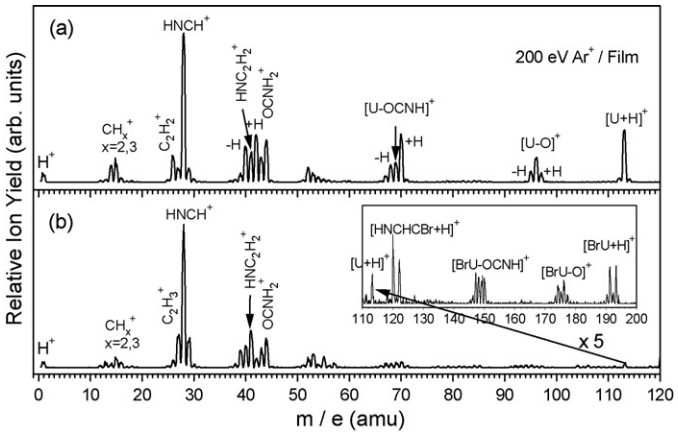

Fig. 3. *Cation* fragment patterns of (a) uracil and (b) 5-BrU produced by 200 eV Ar^+ ion irradiation of 200 ng/cm^2 films on Pt substrate. Again, in both mass spectra the relative intensity of the mass peaks has been normalized to their integral intensity of all fragments. The cation mass spectrum of 5-BrU is completed up to 200 amu in its inset (5×).

(∼1%). Bond cleavage along N1–C6 and C4–C5 yields fragments $C_3H_2^+$ (38 amu), $C_3H_3^+$ (39 amu) and $C_3H_4^+$ (40 amu) from thymine, $C_2H_2^+$ (26 amu) and $C_2H_3^+$ (27 amu) from uracil. In the case of BrU, it produces a negligible fragment C_2HBr^+ at 104 and 106 amu. The 27 amu peak may also have contribution from HCN^+ in all cases.

The peaks between 12 and 14 amu are assignable to hydrocarbon fragments, C^+, CH^+ and CH_2^+. In the case of thymine, these fragments with an additional CH_3^+ at 15 amu are predominantly due to the 5-methyl group, as suggested by the peak shifts of partially deuterated thymine. Here their appearance involves hydrogen abstraction by ring hydrocarbon fragments of uracil and 5-BrU. The H^+ fragment is negligible in all cases.

Fig. 3 shows typical ion stimulated desorption (ISD) mass spectra of *cation* fragments produced by 200 eV Ar^+ ion irradiation of 200 ng/cm^2 (a) uracil and (b) 5-BrU films condensed on Pt. On first sight the mass patterns are quite similar to that produced by 70 eV electron impact in Fig. 2. However, careful examination of the results reveals several differences. First of all, we need to note that during ion irradiation the most abundant fragment at 28 amu is likely due exclusively to the $HNCH^+$ fragment as in the case of thymine where it is found to shift to 29 amu when partially deuterated thymine is irradiated [21]. The contribution from another possible CO^+ fragment is nearly negligible, suggesting closure of its formation channel during ion irradiation in condensed phase. But in the case of electron impact, the CO^+ fragment contributes significantly to the 28 amu peak in all cases.

Second, many fragments appear in their protonated forms, i.e., they pick up a hydrogen from the film during desorption. For example, the molecular parent cations are seen predominantly at 127 amu for $[T+H]^+$, 113 amu for $[U+H]^+$, and (191, 193) amu for $[BrU+H]^+$ (inset), respectively, as well as $HNC_2H_2Br^+$ for 5-BrU at 120 and 122 amu. Some fragments partially pick up hydrogen, e.g., fragments resulting from losing a OCNH group (68–70 amu for uracil, and 146–150 amu for 5-BrU), and fragments from bond-breaking along N1–C2 and C4–C5 ($HNC_3H_4^+[\pm H]$ at 54, 55, 56 amu for thymine, and $HNC_2H_2^+[\pm H]$ at 40–43 amu for uracil). Some other fragments desorb without hydrogen addition, e.g., $HNCH^+$. These results reflect the difference in proton affinity of the individual fragments, and their potential to cause further damage to their surrounding medium via hydrogen abstraction following their creation by ionizing radiation. In this respect, we also note that the formation of the $OCNH_2^+$ fragment at 44 amu from thymine is obvious during both electron impact and ion irradiation, and partially involves its methyl hydrogen [21]. It is negligible here during electron impact of uracil and 5-BrU, but obvious again during ion irradiation. This suggests a possible contribution from hydrogen abstraction from the film by, e.g., an $OCNH^+$ fragment.

The third significant difference is the formation of an additional fragment via loss of an oxygen atom, which is observed during ion impact but not during electron impact. Loss of an O atom (breaking of a C=O bond) yields fragment $[U-O]^+$ at 96 amu for uracil, further loss or gain of a hydrogen atom yields the two adjacent peaks at 95 and 97 amu. A similar channel produces the fragments $[BrU-O]^+[\pm H]$ at 173–177 amu for 5-BrU, and $[T-O]^+[\pm H]$ at 109–111 amu for thymine. This fragmentation channel opens up only to condensed phase thymine but closes to isolated thymine molecules. A similar observation is reported during multiply charged (keVs) ion interaction with isolated and clustered uracil and thymine molecules in gas phase [25]. This suggests that it is likely related to the effect of intermolecular hydrogen bonding formed between the O and N–H atoms of clustered or condensed phase molecules (T, U, and 5-BrU) [26].

Finally, we note in the case of 5-BrU that the relative intensity of the parent cation as well as some other heavy fragments containing Br is significantly reduced with respect to other cation fragments (e.g., $HNCH^+$) compared with the corresponding fragments of thymine and uracil produced through same channels. This is a consequence of introducing Br atom of high electron negativity into the molecule. The effect can be of two aspects. First, introducing a high electron-negativity atom into the molecule may reduce the ionization probability by Ar^+ ions, or the probability for the positive charge to reside on a fragment containing Br. Second, the extra mass of Br may impede the desorption of a heavy fragment containing Br.

Fig. 4 shows typical ISD mass spectra of *anion* fragments produced by 200 eV Ar^+ ion irradiation of 20 ng/cm^2 (a) uracil (U) and (b) 5-BrU films condensed on Pt. The spectra were taken from much thinner films in order to show the parent anions. The anion fragment patterns are quite similar in both cases except for the two peaks at 79, 81 amu in the spectra of 5-BrU. These two peaks correspond to fragments $^{79}Br^-$ and $^{81}Br^-$, observed with a similar intensity reflecting the natural abundance of the two bromine isotopes. The other major anions are H^-, O^-, CN^-, and OCN^- at 1, 16, 26, and 42 amu, respectively. Peaks of smaller intensity observed at 38, 39, 40, and 41 amu are assigned to fragments C–CN^-, $C_3H_3^-$, HNC_2H^-, and OC_2H^-, in accord with the identification of thymine anion fragments.

In all three cases, the parent anions are discernable in their deprotonated forms (with loss of a hydrogen) only from very thin films (20–40 ng/cm^2), i.e., $[U-H]^-$ at 111 amu for uracil,

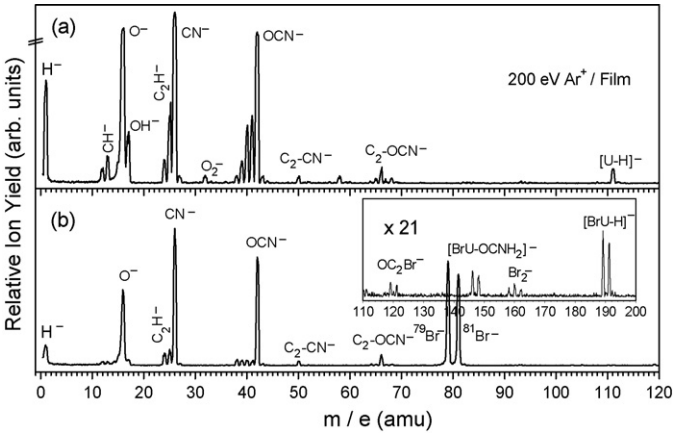

Fig. 4. *Anion* fragment patterns of (a) uracil and (b) 5-BrU produced by 200 eV Ar^+ ion irradiation of 20 ng/cm^2 films on Pt substrate. In both mass spectra the relative intensity of the mass peaks has been normalized to their integral intensity of all fragments. The anion mass spectrum of 5-BrU is completed up to 200 amu in its inset (×21).

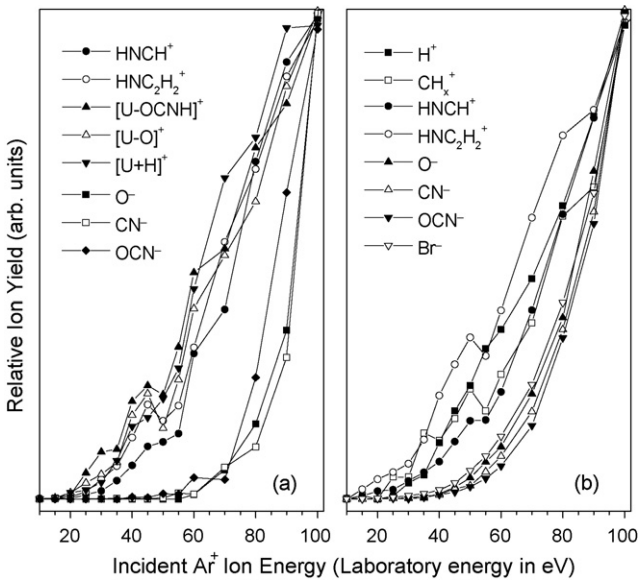

Fig. 5. Relative desorption yields of typical cation and anion fragments as a function of incident ion energy during Ar^+ ion irradiation of (a) uracil and (b) 5-BrU films on Pt. The cation fragments are from 200 ng/cm^2 films, and the anions are from 20 ng/cm^2 films.

$[BrU-H]^-$ at 189, 191 amu (inset) for 5-BrU, and $[T-H]^-$ at 125 amu for thymine, respectively. In the case of thymine, it is further revealed that the hydrogen loss occurs predominantly to the N–H bonds [21], in consistence with a fact that thymine is adsorbed as anion on metal surfaces through the N and O atoms [27–30]. Given their similar molecular structures, it is believed that uracil and 5-BrU molecules may also be adsorbed on the surfaces in a similar way, and thus hydrogen loss are also originated mainly from the N–H bonds.

For 5-BrU, we can also see trace amount of Br_2^- ($^{79}Br_2^-$, $^{79}Br^{81}Br^-$ and $^{81}Br_2^-$ at 158, 160 and 162 amu, respectively), $[BrU-OCNH_2]^-$ (146 and 148 amu), and OC_2Br^- (119 and 121 amu). In all cases, we see C_2CN^- (50 amu) and C_2OCN^- (66 amu) where CN and OCN are from the adsorbed molecules while C_2 likely originates from carbon impurity in Pt substrate. This might also be the case for C–CN^-. Small peaks at 25 and 24 amu may be due to fragments C_2H^- and C_2^- (impurity) while fragments OH^-, CH^-, and C^- may contribute to peaks at 17, 13, and 12 amu. The small OH^- peak at 17 amu is an indication of hydrogen abstraction by oxygen fragments as there is no hydroxyl group in these molecules, which is frequently observed in such experiments. This peak is significantly reduced in the case of 5-BrU due likely to the substitution of H by Br at C5.

Fig. 5 shows the relative desorption yields of major cation and anion fragments as a function of incident Ar^+ ion energy during irradiation of (a) uracil and (b) 5-BrU films. The results for the cations are taken from 200 ng/cm^2 films, and that for the anion fragments from 20 ng/cm^2 films. The data is used to estimate the desorption energy thresholds of the major fragments from uracil and 5-BrU films. Most cation fragments from uracil films (Fig. 5(a)) begin to desorb at energies between 20 eV ($HNCH^+$, $HNC_2H_2^+$, $[U-OCN]^+$, $[U-O]^+$, $[U+H]^+$) and 25 eV (CH_3^+, H^+, not shown). These desorption energy thresholds are close to those of major cation fragments desorbed from thymine and 5-BrU (Fig. 5(b)) films of similar thickness. The fragmentation and desorption dynamics under present conditions have been discussed elsewhere in the cases of thymine and some other biomolecules [23,24]. Fragmentation of uracil and 5-BrU here is believed to follow the same dynamics which involve both potential energy and momentum transfer from an incident ion to a target molecule for the formation of cation fragments.

The anion fragments appear at higher energies at around 50 eV. These values appear to be higher than those for both thymine where H^- appears at 40 eV, CN^- and OCN^- at ~35–40 eV, and 5-BrU where all at ~40 eV. The data of anion fragments is less consistent than that of cation fragments among the three studied base molecules. The latter yields consistent values at around 20 eV. However, an overall trend is that the anion fragments appear at much higher energies than the cation fragments, reflecting a fact that the formation of cation fragments is promoted by the potential energy transfer between an incident ion and a target molecule in terms of both ionization and fragmentation whereas the formation of anion fragments requires more momentum transfer to facilitate fragmentation and (negative) ionization (electron transfer with the film or substrate). Electron transfer (negative ionization) is strongly sensitive to the surface work function, and thus to the adsorption of molecules on the surface in terms of both the coverage and the type of adsorbed molecules.

Much like in the case of thymine, the anion fragment desorption of both uracil and 5-BrU exhibits a strong dependence on the film thickness (coverage) between 20 and 800 ng/cm^2 as shown in Fig. 6 for 5-BrU, in contrast to a less thickness-dependent cation fragment desorption. The relative desorption yields of CN^-, OCN^- and the parent anion $[BrU-H]^-$ decrease sharply with increase in film thickness. The O^- fragment exhibits a somehow reduced sensitivity to the film thickness, while the cation fragments (e.g., $HNCH^+$) show no such significant dependence in the investigated thickness range. The relative lower

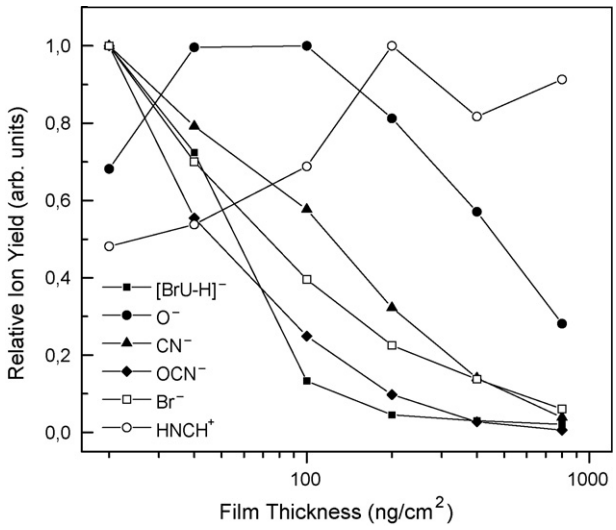

Fig. 6. Film thickness dependence of typical cation and anion fragment desorption yield during 200 eV Ar^+ ion irradiation of 5-BrU films. For clarity, the relative yields are all normalized to their maxima. Note the strong dependence of anion fragment desorption, typically CN^- and OCN^-, on the film thickness.

desorption yield of $HNCH^+$ from low coverage can be ascribed to the fast degradation of the adsorbed molecules. This strong dependence of anion desorption on coverage is ascribed to the change in surface work function caused by molecular adsorption in low coverage regime and a local charging effect at higher coverage. It is also likely responsible for the less consistence in the measured anion desorption energy thresholds among the three base molecules.

We finally have a look at the possible pathways and the consequence of the C5–Br bond cleavage of 5-BrU. Breaking of this bond is likely a result of collision between an incident Ar^+ ion and the Br or C5 atom. There are four possible consequences associated with or without ionization of 5-BrU. In case of ionzation, it can proceed via (a) $BrU^+ \rightarrow U^\bullet + Br^+$, or (b) $BrU^+ \rightarrow U^+ + Br^\bullet$. (a) is very unlikely due to the much higher ionization potential of Br than Ar. This is in consistence with the absence of Br^+ in the mass spectrum of cation fragments. (b) is a possible channel because the resultant $Br^\bullet$ atom may pick up an electron from the film or substrate to appear as Br^-, whereas the resultant U^+ may break into fragments, given the insignificant desorption of U^+ or $[U+H]^+$. Without ionization, it may proceed via (c) dipolar dissociation leading to $BrU \rightarrow U^+ + Br^-$; or (d) homolysis $BrU \rightarrow Uyl^\bullet + Br^\bullet$. Hence, only channel (d) can produce the uracilyl radical that is believed to be responsible for the enhanced radiosensitivity of 5-BrU. The other possible channels (b) and (c) all lead to the formation of a uracil cation followed by its fragmentation.

In terms of the formation of the parent cations, we notice that ionization of the nucleobase molecules in condensed phase by Ar^+ ion impact all ends up with their desorption in protonated forms. This suggests that all these cationic base molecules have high proton-affinities. In addition, we also notice that 70 eV electron ionization of nucleoside thymidine/uridine also leads to the desorption of the base moiety as T^+/U^+ instead of $[T-H]^+/[U-H]^+$ which implies hydrogen abstraction by $[T-H]^+/[U-H]^+$, likely from the sugar moiety [31]. Previously, the enhanced radiosensitivity of 5-BrU has been ascribed exclusively to hydrogen abstraction by *the uracilyl radical* from the sugar moiety of its adjacent 5′-nucleotide [4–12]. The present results lead us to a possible alternative mechanism that involves hydrogen abstraction from the sugar moiety by *the cationic base* of its adjacent 5′-nucleotide. This issue is under further investigation.

4. Summary and conclusion

As part of our effort to unravel possible different molecular level mechanisms of DNA damage caused by heavy ion radiation, and the radiosensitive effect of 5-bromouracil observed during UV, X- and γ-ray irradiation, we have conducted a parallel investigation on ionizing fragmentation of uracil (U), 5-bromouracil (BrU) and thymine (T) by 70 eV electron impact in gas phase and 10–200 eV Ar^+ ion irradiation in condensed phase. Abundant ionic fragments are produced from the three molecules by both electron impact and ion irradiation through similar channels due mainly to their very similar molecular structures. The chemical composition of the charged fragments is then identified according to these similar fragmentation channels.

During electron impact major cation fragments are identified as $[M-OCNH]^+$, $NHCHCCH_3^+$(T)/$NHCHCH^+$(U)/$NHCHCBr^+$(5-BrU), $OCNH_2^+$, $HNCH^+/CO^+$, $C_xH_y^+$ ($x=1$–3; $y=0$–4), etc. as well as a parent cation $[M]^+$, where M = T, U or 5-BrU. During ion irradiation some of these fragments appear predominantly in protonated form, e.g., the parent cations. Some appear partially in protonated form, e.g., fragments resulting from losing an OCNH group and from bond-breaking along N1–C2 and C4–C5 of the molecules. The most abundant $HNCH^+$ fragment desorbs without hydrogen addition. These results reflect the difference in proton affinity of the individual fragments, and bear implications for their potential to cause further damage to their surrounding medium via hydrogen abstraction following their creation by ionizing radiation. An additional fragmentation channel is also open leading to the formation of a cation fragment $[M-O]^+$, which is likely related to the effect of intermolecular hydrogen bonding formed between condensed phase molecules. Major anion fragments produced by ion irradiation include H^-, O^-, CN^-, OCN^- for all the three molecules and an additional Br^- anion for 5-BrU, with trace amount of hydrocarbon anions. During Ar^+ ion irradiation, cation fragment desorption begins at incident ion energies down to ∼20 eV. Anion fragment desorption appears at much higher energies at around ∼40 eV, and strongly depends on the film thickness. The parent anions are discernable in their deprotonated forms only from very thin films.

In terms of the radiosensitive 5-BrU, we note particularly that its fragmentation pattern is quite different from that of thymine and uracil with much less heavy fragments, which we believe is due to the introduction of Br into the molecule. Another finding is the high proton affinity of ionized base molecules, which may bear the causes of the radiosensitivity of 5-BrU. This issue is under further investigation.

Acknowledgements

This work is continuously supported by the Natural Science and Engineering Research Council of Canada, and Canadian Space Agency.

References

[1] X. Hu, H. Li, J. Ding, S. Han, Biochemistry 43 (2004) 6361.
[2] See, e.g.: T.J. Kinsella, P.P. Dobson, J.B. Mitchell, A.J. Fornace Jr., Int. J. Radiat. Oncol. Biol. Phys. 13 (1987) 733.
[3] M.D. Prados, C. Scott, H. Sandler, J.C. Buckner, T. Phillips, C. Schultz, R. Urtasun, R. Davis, P. Gutin, T.L. Cascino, H.S. Greenberg, W.J. Curran Jr., Int. J. Radiat. Oncol. Biol. Phys. 45 (1999) 1109.
[4] F. Hutchinson, Q. Rev. Biophys. 6 (1973) 201.
[5] H. Sugiyama, Y. Tsutsumi, I. Saito, J. Am. Chem. Soc. 112 (1990) 6720.
[6] H. Sugiyama, K. Fujimoto, I. Saito, J. Am. Chem. Soc. 117 (1995) 2945.
[7] H. Sugiyama, Y. Tsutsumi, K. Fujimoto, I. Saito, J. Am. Chem. Soc. 115 (1993) 4443.
[8] T. Chen, G.P. Cook, A.T. Koppisch, M.M. Greenberg, J. Am. Chem. Soc. 122 (2000) 3861.
[9] G.P. Cook, M.M. Greenberg, J. Am. Chem. Soc. 118 (1996) 10025.
[10] T. Watanabe, T. Bando, Y. Xu, R. Tashiro, H. Sugiyama, J. Am. Chem. Soc. 127 (2005) 44.
[11] H. Abdoul-Carime, M.A. Huels, E. Illenberger, L. Sanche, J. Am. Chem. Soc. 123 (2001) 5354.
[12] H. Abdoul-Carime, M.A. Huels, F. Brüning, E. Illenberger, L. Sanche, J. Chem. Phys. 113 (2001) 2517.
[13] S. Cecchini, S. Girouard, M.A. Huels, L. Sanche, D.J. Hunting, Biochemistry 44 (2005) 1932.
[14] S. Cecchini, C. Masson, C. La Madeleine, M.A. Huels, L. Sanche, J.R. Wagner, D.J. Hunting, Biochemistry 44 (2005) 16957.
[15] J. de Vries, R. Hoekstra, R. Morgenstern, T. Schlathölter, Phys. Rev. Lett. 91 (2003) 053401.
[16] T. Schlathölter, R. Hoekstra, S. Zamith, Y. Ni, H.G. Muller, M.J.J. Vrakking, Phys. Rev. Lett. 94 (2005) 233001.
[17] T. Schlathölter, R. Hoekstra, R. Morgenstern, Int. J. Mass Spectrom. 233 (2004) 173.
[18] Z.-W. Deng, I. Bald, E. Illenberger, M.A. Huels, Phys. Rev. Lett. 95 (2005) 153201.
[19] Z.-W. Deng, I. Bald, E. Illenberger, M.A. Huels, Phys. Rev. Lett. 96 (2006) 243203.
[20] Z.-W. Deng, I. Bald, E. Illenberger, M.A. Huels, J. Chem. Phys., submitted for publication.
[21] M. Imhoff, Z.-W. Deng, M.A. Huels, Int. J. Mass Spectrom. 245 (2005) 68.
[22] Z.-W. Deng, M. Imhoff, M.A. Huels, J. Chem. Phys. 123 (2005) 144509.
[23] I. Bald, Z.-W. Deng, E. Illenberger, M.A. Huels, Phys. Chem. Chem. Phys. 8 (2006) 1215.
[24] M. Imhoff, Z.-W. Deng, M. Rajabian, F. Brüning, M.A. Huels, in preparation.
[25] T. Schlathölter, F. Alvarado, S. Bari, A. Lecointre, R. Hoekstra, V. Bernigaud, B. Manil, J. Rangama, B. Huber, Chem. Phys. Chem. 7 (2006) 2339.
[26] R.E.A. Kelly, L.N. Kantorovich, J. Phys. Chem. B 110 (2006) 2249.
[27] M. Furukawa, H. Fujisawa, S. Katano, H. Ogasawara, Y. Kim, T. Komeda, A. Nilsson, M. Kawai, Surf. Sci. 532 (2003) 261.
[28] A. McNutt, S. Haq, R. Raval, Surf. Sci. 502 (2002) 185.
[29] W.-H. Li, W. Haiss, S. Floate, R.J. Nichols, Langmuir 15 (1999) 4875.
[30] W. Haiss, B. Roelfs, S.N. Port, E. Bunge, H. Baumgärtel, R.J. Nichols, J. Electroanal. Chem. 454 (1998) 107.
[31] S. Ptasińska, P. Candori, S. Denifl, S. Yoon, V. Grill, P. Scheier, T.D. Märk, Chem. Phys. Lett. 409 (2005) 270.